İSTANBUL UNIVERSITY CERRAHPAŞA

ORIGINAL ARTICLE
Electrica 2023; 23(3): 522-533

Artificial Eco-System-Based Optimization Algorithm for Optimal Design of Single-Machine Infinite Bus and Multi-Machine Power System Stabilizers

Aliyu Sabo[1], Theophilus Ebuka Odoh[2], Noor Izzri Abdul Wahab[1]

[1]Department of Electrical and Electronics Engineering, University Putra Malaysia, Advanced Lightning, Power and Energy Research (ALPER), Serdang, Malaysia
[2]Department of Electrical/Electronics Engineering, Nigerian Defence Academy, Kaduna, Nigeria

Cite this article as: T. Ebuka Odoh, A. Sabo, N. Izzri Abdul Wahab and H. Beiranvand, "Artificial eco-system-based optimization algorithm for optimal design of single-machine infinite bus power system stabilizer," *Electrica*, 23(3), 522-533, 2023.

ABSTRACT

This research evaluates the viability of the artificial eco-system optimization (AEO), a novel metaheuristic algorithm, for optimal power system stabilizers (PSSs) tuning in single-machine infinite bus (SMIB) and western system coordinating council (WSCC) multi-machine power systems. The PSS design problem was converted to an optimization problem to achieve optimal tuning, and an eigenvalue-based objective function was employed. The eigenvalue objective function was defined to optimally obtain the PSSs parameters and enhance the power system dynamic performance by improving the damping of electromechanical modes (EMs). The proposed AEO-based PSS performance was validated by comparing the results obtained with genetic algorithm (GA)-based PSS, particle swarm optimization (PSO)-based PSS design, and similar published work. AEO-based PSS method of tuning has been shown to damp electromechanical modes (EMs), control low-frequency oscillations (LFO), and provide better transient performance and convergence rate.

Index Terms—Artificial eco-system optimization, oscillation damping, power system dynamic stability, power system stabilizer.

I. INTRODUCTION

Low-frequency oscillations (LFO) is a significant issue in the operation of power grid system because they threaten the stability and integrity of the grid if not adequately controlled. This control is essential, particularly in current power grid systems, as the interconnection of power systems keeps increasing to meet the energy demand [1]. Controlling LFOs in the power grid system also helps to improve the power transfer capability and achieve stabilization in the system. Stabilization requires taking care of small-signal stability, which involves LFOs. Damping controllers such as power system stabilizers (PSSs) are used to improve the damping of electromechanical modes (EMs), thereby controlling LFOs in single-machine and multi-machine systems. Power system stabilizers compensate for the lag error between the generator excitation input and electrical torque and generate an additional torque on the rotor [2].

Though the power system is nonlinear, the PSS design is based on the linear control theory via a linearized model of the power system. PSS parameters are tuned about a defined operating point in the linearized model. Nonlinearity in power system means spontaneous continuous fluctuations over a wide operating range. More so, power system configuration changes with time due to these fluctuations and thus requires the adjustment of PSS parameters to maintain a stable working condition. This makes conventional PSS with fixed parameters unreliable in providing optimal performance over the entire operating condition.

Different control techniques for PSS design include pole placement and shifting, feedback control loop, and self-tuning regulators. These techniques have limitations of low intensive computation efficiency and extended information processing time.

In PSS design for single-machine and multi-machine power systems, several meta-heuristic techniques have been proposed as viable ways for offline tuning of PSS. These proposals were done by considering a wide operating condition region. Some of the techniques include farmland

Corresponding author:
Theophilus Ebuka Odoh

E-mail:
theophilusodh@gmail.com

Received: December 14, 2022

Accepted: March 8, 2023

Publication Date: August 1, 2023

DOI: 10.5152/electrica.2023.22228

fertility algorithm [3–5], Henry gas solubility optimization [2], kidney-inspired algorithm [6], general relativity search algorithm [7], sine cosine algorithm [8], modified arithmetic optimization [9], artificial gorilla troops optimization [10], cuckoo search optimization [11], and Harris hawk optimization [12]. Improved grey wolf and differential evolution algorithm was used in proportional integral derivative (PID) and fractional PSS in [13]. A modified differential evolutionary particle swarm optimization algorithm was used to design PSS in hydro system in [14] and a modified differential evolutionary algorithm was also used to design PSS in [15] considering solar penetration. Metaheuristic algorithms have also been adopted in other damping controller designs like flexible alternating current transmission systems (FACTS). A new hybrid differential evolution with whale optimization algorithm was used for fractional static synchronous series compensator and governor design in solar photovoltaic, wind, and hydro systems in [16], and grey wolf optimization was adopted in interline power flow controller (IPFC) design in study [17]. The significant advantage of deploying metaheuristic techniques is the ability to escape local minima and explore a global solution to the optimization problem.

Artificial eco-system optimization (AEO) is a novel meta-heuristic algorithm developed to solve complex optimization [18]. AEO optimization has been applied in various applications, such as parameter estimation of solar photovoltaic models [19] in PID controller design for buck converter [20] and economic emission dispatch [21]. However, there are still emerging engineering problems that AEO can be adopted to solve and further evaluate its efficiency. Thus, this research evaluates the viability of the new algorithm for a recent engineering problem by assessing AEO viability for optimal tuning of PSS in a single- and multi-machine power system for the first time.

This research was carried out by defining the PSS damping controller problem as an optimization problem and AEO was applied for PSS tuning. An eigenvalue objective function was formulated to improve the stability of single-machine infinite bus (SMIB) and Western System Coordinating Council (WSCC) by improving the damping of electromechanical modes and also obtain the gains and parameters of the stabilizers. Nonlinear time-domain simulation results and transient performance analysis indicate the efficiency of the proposed AEO–PSS damping controller as validated via comparison with genetic algorithm, particle swarm optimization-based PSS, and similar published work.

II. ARTIFICIAL ECO-SYSTEM OPTIMIZATION (AEO)

Artificial eco-system is a nature-inspired novel metaheuristic algorithm developed by [18]. The algorithm imitates the flow of energy between the three unique components in an eco-system and their behavioral processes, which are the producer (production), the consumer (consumption), and the decomposer (decomposition). The interaction between these three components makes up an ecosystem food chain, which describes the feeding process in an eco-system and shows the flow of energy in an eco-system. Only one producer and one decomposer exist as an individual in the eco-systems population. The rest of the population, representing the search space, are consumers chosen as carnivores, herbivores, or omnivores with the same probability. Fig. 1 depicts the energy flow in an eco-system.

A. Production Process

The production process allows AEO to randomly produce a new search entity. The produced new search entity displaces the former one known as the best entity (solution) (x_n). This displacement is between the best entity and a new search entity randomly produced in the search space $\left(x_{rand}\right)$. An operator known as production operator is used to mathematically describe the equations (1)–(3) as follows:

$$x_1(t+1)=(1-a)x_n(t)+ax_{rand}(t) \tag{1}$$

$$a=\left(1-\frac{t}{maxit}\right)r_1 \tag{2}$$

$$x_{rand}=r.\left(V_{PSS}^{max}-V_{PSS}^{min}\right)+V_{PSS}^{min} \tag{3}$$

where the population size is represented by n, the maximum number of iterations performed or the stop criteria is given as $maxit$, V_{PSS}^{max} and V_{PSS}^{min} are the upper PSS and lower PSS limits, respectively, and r_1 is value randomly generated in the range of [0,1]. r is a vector produced randomly within the range of [0,1], linear weighting coefficient is given as a, and x_{rand} is an individual position produced randomly in search space.

B. Consumption Process

After the production process, consumption takes place by the consumers. Each consumer in order to obtain food energy, may either feed on a consumer randomly chosen with lower energy level, a producer or both. A consumption factor with levy flight characteristics

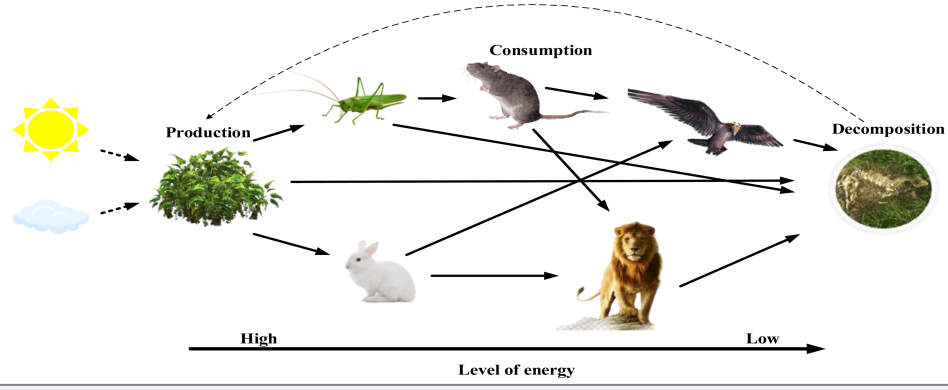

Fig. 1. Diagram representing energy flow in an eco-system.

is proposed and defined in equations (4) and (5) as a simple parameter-free random walk.

$$C = \frac{1}{2}\frac{v_1}{|v_2|} \tag{4}$$

$$v_1 \in N(0,1), v_2 \in N(0,1) \tag{5}$$

where normal distribution is given as $N(0,1)$ with standard deviation as 1 and mean = 0.

Consumption factor is crucial because it assists each consumer in hunting for food. The three consumers, carnivores, herbivores, and omnivores, adopt unique consumption strategies.

If a herbivore is randomly selected as a consumer, it can only eat the producer. Its behavior is represented in a mathematical model as shown in equation (6):

$$x_i(t+1) = x_i(t) + C.(x_i(t) - x_1(t)), \quad i \in [2,\ldots,n] \tag{6}$$

However, if a consumer randomly chosen is an carnivore, it can feed only on a random consumer with a higher energy level and can be mathematically modeled in equation (7) as follows:

$$x_i(t+1) = x_i(t) + C.(x_i(t) - x_j(t)), \quad i \in [3,\ldots,n], \tag{7}$$

$$j = randi([2i-1]) \tag{8}$$

Also, if an omnivore is randomly selected as a consumer, the omnivore can feed on a random consumer with a higher energy level and a producer as well. It is mathematically modeled in equations (9) and (10) as follows:

$$x_i(t+1) = x_i(t) + C.(r_2.(x_i(t) - x_1(t)) + (1-r_2)(x_i(t) - x_j(t))), \quad i = 3,\ldots,n \tag{9}$$

$$j = randi([2i-1]) \tag{10}$$

where r_2 is a number generated randomly in range of [0, 1].

C. Decomposition Process

The decomposition process is essential because it provides the producer with the required nutrients for growth. The decomposer chemically breaks down the remains of each individual in the population after death. Its behavior is mathematically modeled using a decomposition factor D with weighting coefficients e and h in (11)–14 as follows:

$$x_i(t+1) = x_n(t) + D.(e.x_n(t) - h.x_i(t)) \quad i = 1,\ldots,n \tag{11}$$

$$D = 3u, \quad u \in N(0,1) \tag{12}$$

$$e = r_3.randi([12]) - 1 \tag{13}$$

$$h = 2.r_3 - 1 \tag{14}$$

Fig. 1 shows the flow of energy in an eco-system.

The steps of the AEO algorithm for optimal PSS tuning are as follows:

1. Initialize a search space randomly in an eco-system. Each obtained solution is defined by a vector, x, $x = [K_P, T_1, T_2, T_3, T_4]$ in the PSS controller.
2. Calculate each eco-system energy level via the objective function equation (26) and update the best solution.
3. Production process: using equation (1), update the position for individual x_1.
4. Consumption process: each consumer has the same probability of selection; hence, for individuals $x_2 \ldots x_n$, its position is updated using equation (6) if the selected individuals are herbivores, if the selected individual are carnivores, individual position is updated using equation (7) and using if they are omnivores Equation (9) is deployed.
5. Calculate each eco-system energy level via equation (26) and update the result as best solution.
6. Decomposition process: each position is updated using equation (11).
7. Calculate each eco-system energy level via the objective function equation (26) and update the best solution.
8. Repeat steps 3–7 until the stop criteria is reached which is the maximum number of iterations.
9. Population with a higher flow of energy is chosen as the best or optimal solution.

Fig. 2 shows the AEO flow chart for the described procedure above in PSS parameter tuning.

III. PROBLEM FORMULATION

A. Power System Model

The power system dynamic model is described using differential algebraic equations (DAEs) [22] and are used to represent a power system with *m* number of synchronous machine and the voltage regulator called automatic voltage regulator (AVR). The DAEs are as described in equations (15–20) [3]:

$$T'_{d0i}\frac{dE'_{qi}}{dt} = -E'_{qi} - (X_{di} - X'_{di})I_{di} + E_{fdi} \tag{15}$$

$$T'_{q0i}\frac{dE'_{di}}{dt} = -E'_{di} - (X_{qi} - X'_{qi}) \tag{16}$$

$$\frac{d\delta_i}{dt} = \omega_i - \omega_s \tag{17}$$

$$\frac{2H_i}{\omega_s}\frac{d\omega_i}{dt} = T_{Mi} - E'_{di}I_{di} - E'_{qi}I_{qi} - (X_{di} - X'_{di})I_{di}I_{qi} - D_i(\omega_i - \omega_s) \tag{18}$$

$$T_{Ai}\frac{dE_{fdi}}{dt} = -K_{Ai}E_{fdi} + K_{Ai}(V_{refi} - V_i) \tag{19}$$

where in equations (15–19) subscript i denotes *i*th synchronous generator, T'_{d0} and T'_{q0} are the *d*-axis and *q*-axis open-circuit time constants, E'_d and E'_q are the transient Electromagnetic Field (EMF) of the *d*-axis and *q*-axis due to flux linkage in the damper coils, E_{fd} is the excitation field voltage, X_d and X_q are the synchronous transient and sub-transient of *d*-axis and *q*-axis reactances, respectively, δ is the rotor angle of the generator, ω is the generator rotor speed, ω_s is the generator synchronous speed, H is the generator inertia constant, D is the damping coefficient, T_M is the mechanical torque or power output, I_d and I_q are stator current *d*-axis and *q*-axis

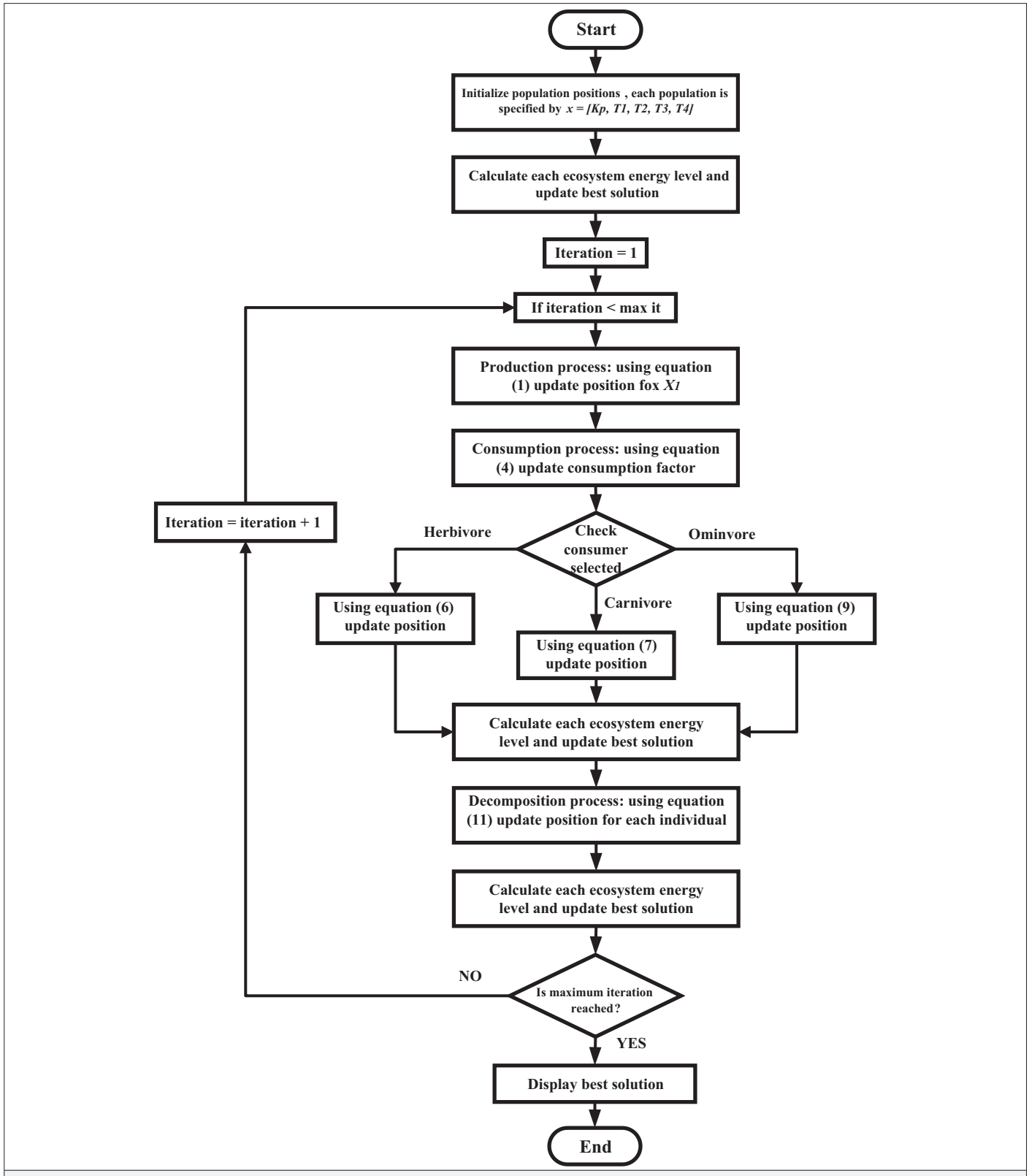

Fig. 2. Flowchart of an artificial eco-system optimization algorithm.

components, respectively, V_{ref} is the reference excitation voltage, V is the terminal voltage of generator, K_A is excitation static gain, T_A is the regulator time constant, T_E is the electrical torque, V_d and V_q are generator terminal voltage of the *d*-axis and *q*-axis components, and R_s is the armature resistance.

T_{Mi}, the input mechanical torque, is kept constant while designing the excitation controller, i.e., to not significantly affect machine dynamics, the generator action is assumed to be slow. Electrical torque is described and substituted in equation (18) as follows:

$$T_{Ei} = E_{di}^{'} I_{di} + E_{di}^{'} I_{di} + \left(X_{qi}^{'} - X_{di}^{'}\right) I_{di} I_{qi} \tag{20}$$

A power grid system with *n* number of buses and *m* number of generators, load buses *m*–*n* are described using algebraic equations as follows from equations (21–23):

$$0 = V_i e^{j\theta i} + \left(R_{si} + jX_{di}^{'}\right)\left(I_{di} + jI_{qi}\right) e^{j\left(\delta i - \frac{\pi}{2}\right)} - \left[E_{di}^{'} + \left(X_{qi}^{'} - X_{di}^{'}\right) I_{qi} + jE_{qi}^{'}\right] e^{j\left(\delta i - \frac{\pi}{2}\right)}$$

$$i = 1, \ldots, m \tag{21}$$

$$V_i e^{j\theta i}\left(I_{di} + jI_{qi}\right) + P_{Li}\left(V_i\right) + jQ_{Li}\left(V_i\right) = \sum_{k=1}^{n} V_i V_k Y_{ik} e^{j(\theta i - \theta k - \alpha_{ik})}, i = 1, \ldots, m \tag{22}$$

$$P_{Li}\left(V_i\right) + jQ_{Li}\left(V_i\right) = \sum_{k=1}^{n} V_i V_k Y_{ik} e^{j(\theta i - \theta k - \alpha_{ik})}, i = m+1, \ldots, n \tag{23}$$

The load active power and reactive power are represented by P_L and Q_L, respectively. Yej–. denotes the power system admittance matrix and θ is the bus voltage V angle. The admittance matrix load element in power lines is reduced by the order reduction method, as in equation (24).

$$\Delta x = A\dot{x} + Bu, \tag{24}$$

The power system linear model is described using equation (24), where x is the system state vector variables, A is the state space matrix of the system, B is the system input matrix, and u is the system control input vector.

B. PSS Design Procedure

This research makes use of the conventional lead–lag PSS connected to the excitation system IEEE-ST1 type for analysis [23], as shown in Fig. 3; the figure also connects an SMIB test system. The *i*th system transfer function in equation (25) describes the PSS connection with IEEE-ST1 excitation system as follows [24]:

$$G_i\left(s\right) = \frac{V_{PSSi(s)}}{\Delta w_i\left(s\right)} = K_{Gi} \frac{T_w s}{\left(1 + sT_w\right)} \frac{\left(1 + sT_{1i}\right)}{\left(1 + sT_{2i}\right)} \frac{\left(1 + sT_{3i}\right)}{\left(1 + sT_{4i}\right)} \tag{25}$$

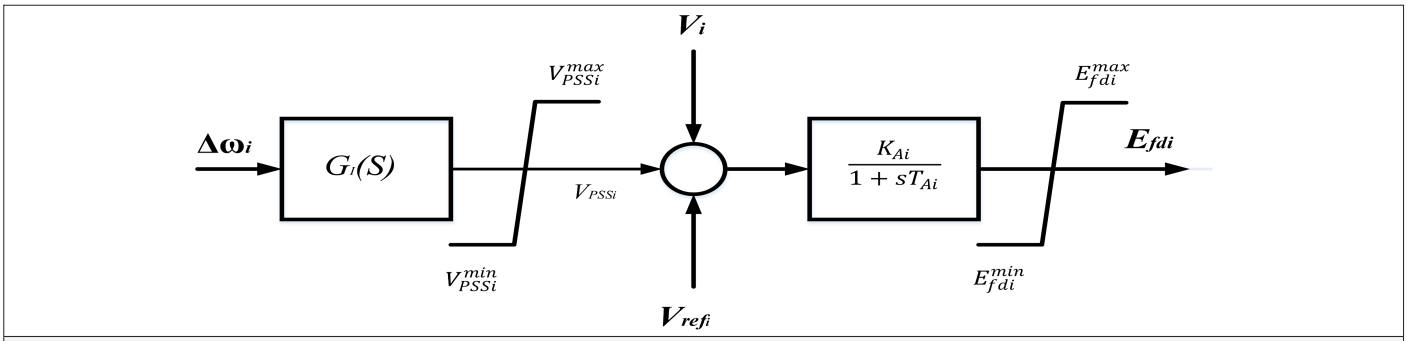

Fig. 3. Connection between a conventional power system stabilizer (PSS) and IEEE--ST1-type excitation system [4].

TABLE I. PARAMETER SETTING FOR THE GA, PSO, AND AEO ALGORITHMS

Parameters	GA	PSO	AEO
Maximum iterations	100	100	100
Population size	100	100	100
Simulation time =10 s Simulations = 20	*mutation rate* = 0.02, *Beta* = 1, *gamma* = 0.1	*inertia weight* $(w) = 1$, *weight damping ratio* $(wdamp) = 0.99$, $C_1 = 1.5, C_2 = 2.0$	*Damping factor* $(D) = 3u$ *where* $u \sim N(0,1)$, *weight coefficients* $(h,e)\ h = 2$, *Consumption factor* $C = \frac{1}{2}\frac{v_1}{\lvert v_2 \rvert}$
Lower limits	$K_{pss}, T_1, T_2, T_3, T_4 = 0.001, 0.001, 0.02, 0.001, 0.02$		
Upper limits	$K_{pss}, T_1, T_2, T_3, T_4 = 50, 1, 1, 1, 1$		

AEO, artificial eco-system optimization; GA, genetic algorithm; PSO, particle swarm optimization.PSS gain (KPSS) and parameters (T1, T2, T3, and T4) constraints

TABLE II. MACHINE DATABASE VALUES OF THE SMIB MODEL

Transmission line	$X_T = 0.0625pu, X_L = 0.2pu$
Machine	$H = 6.4s, D = 0.0, T'_{d0} = 6.0s, T'_{q0} = 0.535s, X_q = 0.8645, X_d = 0.8958, X'_q = 0.1969s, X'_d = 0.1198s$
Exciter	$K_A = 50.0, T_A = 0.05s$
Operating point information	$P_G = 1.63pu, V_1 = 1.026pu, V_2 = 1.025pu$

T'_{d0} and T'_{q0} are the *d*-axis and *q*-axis open-circuit time constants, X_d and X_q are the synchronous transient and sub-transient of *d*-axis and *q*-axis reactances, respectively, H is the generator inertia constant, D is the damping coefficient, P_G is the power output, V_1 is the terminal voltage of generator, K_A is the excitation static gain, T_A is the regulator time constant, X_T is the transmission line reactance, and X_L is the inductance of the transmission line.
SMIB, single-machine infinite bus.

where the output signal of the PSS at the *i*th machine is V_{PSSi}, T_w is the washout time constant equal to 10 in this study, and the *i*th machine synchronous speed deviation signal is Δw_i. Optimal parameters of stabilizer gain K_{Gi} and parameters T_{1i}, T_{2i}, T_{3i}, and T_{4i} are to be determined.

C. PSS Design Results

1) Objective Function Formulation and Performance Indices for Error Minimization

In [25, 26], the authors explained the single- and multiple-objective function. This research adopted a single-objective function. Rotor speed deviation error results in electromechanical modes of oscillation; therefore, to improve the damping of these electromechanical modes, which minimizes the rotor speed deviation error, the damping ratio is maximized for faster oscillation attenuation. The eigenvalue single-objective function was employed to enhance the damping characteristics of electromechanical modes in the system and shift the eigenvalues of the power system to the left region of complex s-plane. Stabilizer gain and parameters of the PSS are determined through the defined eigenvalue objective function as shown in equation (26):

$$J_{eig} = \max\left\{real(\lambda_i) \mid \lambda_i \int EMs\right\} + P_C \sum\left\{real(\lambda_j) \mid \lambda_j > 0\right\}$$

$$EMs = \left\{\lambda_k \mid 0 < \frac{im(\lambda_k)}{2\pi} < 5\right\} \quad (26)$$

Eigenvalues of the power system state space matrix are denoted by λ_i, and P_C is a penalty constant applied for producing the positive eigenvalues and enhancing slow eigenvalues [23]. In this study the single objective function which accesses the error performance. J_{eig}, which is the objective function, is minimized subject to PSS gain (K_{Gi}) and parameters (T_{1i}, T_{2i}, T_{3i}, and T_{4i}) with constraints $0.001 \le K_{Gi} \le 50$ and $0.001 \le T_{1i} \le 1$, $0.02 \le T_{2i} \le 1$, $0.001 \le T_{3i} \le 1$, and $0.02 \le T_{4i} \le 1$ [7]. The AEO algorithm proposed for PSS design computes the defined optimization problem using the objective function and constraints to obtain optimal values. Table III also shows the unstable damping ratios for no-PSS and the optimized damping ratio for AEO-PSS, PSO-PSS, and GA-PSS with their corresponding frequencies.

2) Single-Machine Infinite Bus

Here, an SMIB test power system is considered [22]. Fig. 5 shows the single-line diagram of the SMIB, whose result was evaluated using GA-based PSS and PSO-based PSS [5]. The optimization process was terminated after 100 iterations for all three algorithms in a population search space of 100. All three methods were performed 20 times before optimal PSS parameters were chosen. Table I shows the parameter settings for all three optimization algorithms performed on the SMIB system.

The SMIB model is described using DAEs in equations (15–20). The dynamic parameters of the SMIB power system are given in Table II [22]. This research used the MATPOWER toolbox to compute the power flow of the system and its initial conditions. The DAEs in the power system model are solved via an ODE solver in MATLAB/SIMULINK. Table II also shows the machine database values of the SMIB model.

3) SMIB Test Power system Time-Domain Simulation without PSS Damping Controller

The test system with no system loading change is simulated under a disturbance. Eigenvalues and nonlinear time-domain analysis simulation were conducted under a 100 ms symmetrical three-phase fault observed at t =1s. The fault was cleared after t = 0.2s and the system's stable condition was restored, Table III shows the unstable damping ratios for No-PSS and the optimized damping ratio for AEO-PSS, PSO-PSS and GA-PSS with their corresponding frequencies, this the single objective function which accesses the error performance

TABLE III. DAMPING RATIO PERFORMANCE INDEX WITH CORRESPONDING FREQUENCY

No-PSS		AEO-PSS		PSO-PSS		GA-PSS	
Damping Ratio	**Frequency**	**Damping Ratio**	**Frequency**	**Damping Ratio**	**Frequency**	**Damping Ratio**	**Frequency**
–0.0070	1.3306	**0.6583**	2.0068	**0.4285**	1.5859	**0.3771**	1.8146
–0.0070	1.3306	**0.8367**	1.1487	**0.6128**	0.9703	**0.6668**	0.8259

AEO, artificial eco-system optimization; GA, genetic algorithm; PSO, particle swarm optimization; PSS, power system stabilizer.

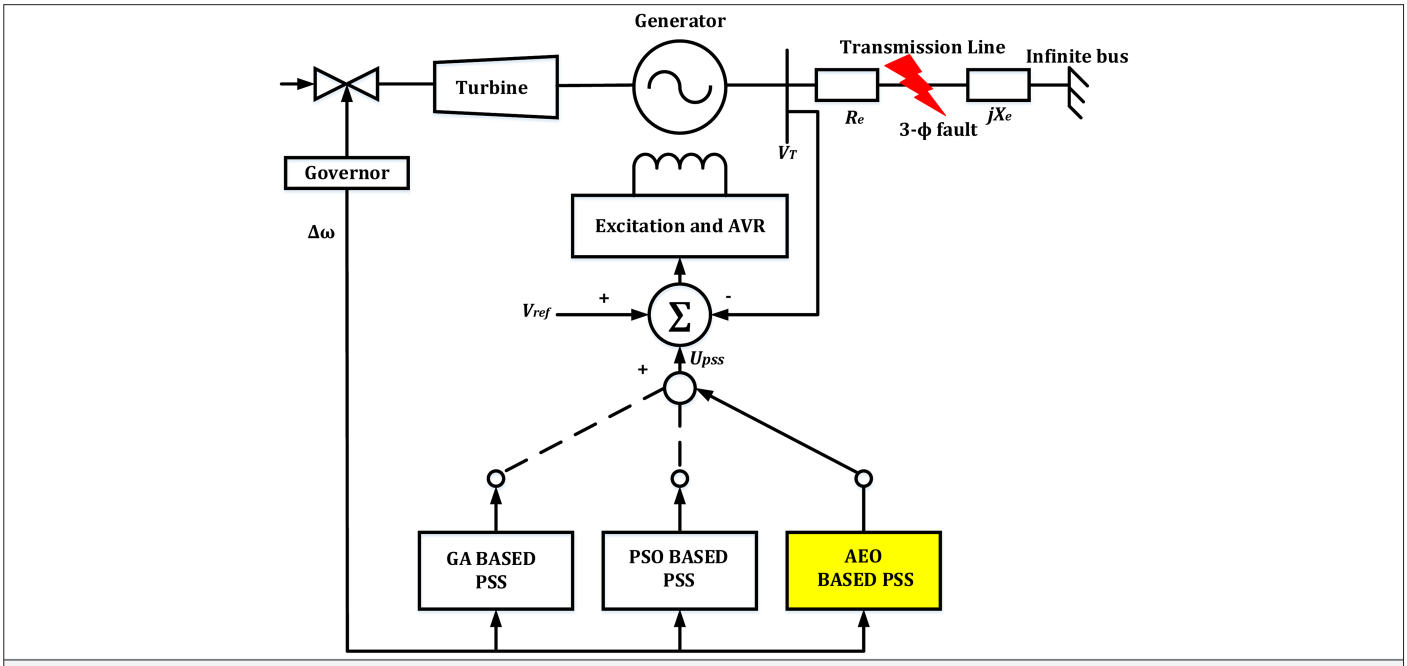

Fig. 4. Schematic diagram of SMIB with AVR and excitation in power system. AEO, artificial eco-system optimization; AVR, automatic voltage regulator; GA, genetic algorithm; PSO, particle swarm optimization; PSS, power system stabilizer; SMIB, single-machine infinite bus.

TABLE IV. PSS OPTIMAL PARAMETERS USING GA, PSO, AND AEO SEARCH ALGORITHMS

Algorithm	K_G	T_1	T_2	T_3	T_4
GA	8.9429	0.5499	0.6597	0.5293	0.0200
PSO	4.6824	0.7697	0.5810	0.5366	0.0201
AEO	39.6109	0.0984	0.0200	0.0949	0.0200

PSS gain (KG) and time constants (T1, T2, T3, and T4) constraints.
AEO, artificial eco-system optimization; GA, genetic algorithm; PSO, particle swarm optimization; PSS, power system stabilizer.

indices in the design. The nonlinear time domain results are shown in Table V. Table V indicates eigenvalue results and corresponding damping ratio and frequency for the case without PSS installed on the power system and with AEO, GA,and PSO- based PSS installed on the power system. A weak damping ratio at Mode 1 with no PSS and corresponding eigenvalues of $0.0588 \pm j8.3601$ is observed from Table V. Also, -0.0070 is noted as the worst electromechanical mode damping ratio.

4) SMIB Test Power System Time-Domain Simulation with AEO-PSS, GA-PSS, and PSO-PSS Damping Controller

In PSS design, the operating conditions used without PSS case were still adopted where a 100 ms symmetrical three-phase fault was

TABLE V. THE SMIB POWER SYSTEM EIGENVALUE RESULTS AND ITS CORRESPONDING ELECTROMECHANICAL MODE DAMPING RATIO FOR GA, PSO, AND AEO-PSS

Mode	No-PSS	GA-PSS	PSO-PSS	AEO-PSS
		Eigenvalue, damping ratio		
1	$0.0588 \pm j8.3601, -0.0070$	$-4.6415 \pm j11.4012, 0.3771$	$-4.7259 \pm j9.9642, 0.4285$	$-11.0256 \pm j12.6091, 0.6583$
2	$-13.2994 + j0.0000, 1.0000$	$-4.6435 \pm j5.1892, 0.6668$	$-4.7280 \pm j6.0965, 0.6128$	$-11.0256 \pm j7.2176, 0.8367$
3	$-8.8414 + j0.0000, 1.0000$	$-0.1005 + j0.0000, 1.0000$	$-0.1003 + j0.0000, 1.0000$	$-0.1025 + j0.0000, 1.0000$
4	$-3.0673 + j0.0000, 1.0000$	$-1.5078 + j0.0000, 1.0000$	$-3.2732 + j0.0000, 1.0000$	$-2.1881 + j0.0000, 1.0000$
5		$-3.2179 + j0.0000, 1.0000$	$-1.7255 + j0.0000, 1.0000$	$-8.1633 + j0.0000, 1.0000$

δ is the rotor angle of the generator, ω is the generator rotor speed, E_{fd} is the excitation field voltage, and E_q' is the transient EMF q-axis due to flux linkage in the damper coils.
AEO, artificial eco-system optimization; GA, genetic algorithm; PSO, particle swarm optimization; PSS, power system stabilizer; SMIB, single-machine infinite bus.

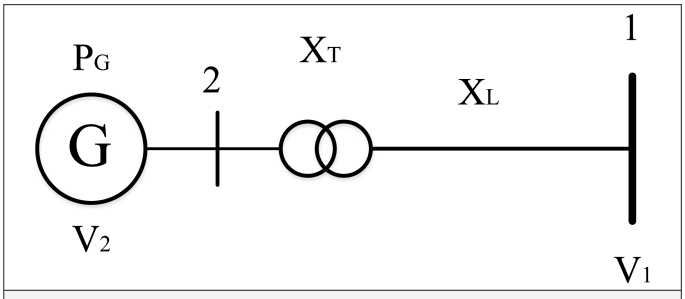

Fig. 5. Single-machine infinite bus (SMIB) line diagram [20]. Convergence curves of AEO, PSO, and GA in obtaining optimal PSS design. AEO, artificial eco-system optimization; GA, genetic algorithm; PSO, particle swarm optimization; PSS, power system stabilizer.

TABLE VI. SMIB SYSTEM PSS-OPTIMIZED PARAMETER COMPARISON WITH STUDY [9]

	Proposed Model	**Reference Model [9]**
Parameters	**AEO-PSS**	**mAOA-PSS**
K_G	39.6109	42.9745
T_1	0.0984	0.08039
T_2	0.0200	0.01023
T_3	0.0949	0.07818
T_4	0.0200	0.01015
No-PSS	AEO-PSS	mAOA-PSS
$0.0588 \pm j8.3601, 0.7\%$	$11.0256 \pm j12.6091, 65.83\%$	$2.6040 \pm j4.0211, 54.36\%$

AEO, artificial eco-system optimization; PSS, power system stabilizer; SMIB, single-machine infinite bus; mAOA, modified arithmetic optimization algorithm.

observed at $t = 1s$ to show the importance of PSS. A nonlinear time-domain simulation was also performed using the AEO algorithm for PSS design, and the AEO performance was validated by comparing it with GA-based PSS and PSO-based PSS, and a similar work carried out by [9]. An eigenvalue objective function was employed as described in equation (26) to increase the electromechanical modes damping properties of PSS, where control parameters of the PSS are determined by computing the system state space matrix A from equation (24). PSS parameters obtained are also shown in Table IV.

PSS parameters obtained in Table IV were used for time-domain simulations. The results of eigenvalues and their corresponding damping ratio for the SMIB test power system with AEO-, GA-, and PSO-based applied to the power system, respectively, is shown also in Table V. From Table V, mode 1 produced a weak damping ratio for electromechanical mode in no-PSS. Following an optimal PSS-based design, mode 1 was impressively enhanced from $0.0588 \pm j8.3601$ to stable mode of $-11.0256 + j12.6091$ for AEO-PSS, $-4.6415 - j11.4012$ for GA-PSS, and $-4.7259 - j9.9642$ for PSO-PSS, respectively. Relatively, the EM worst damping ratio -0.0070 was enhanced to 0.6583 for AEO-PSS, 0.3771 for GA-PSS, and 0.4285 for PSO-PSS, respectively.

TABLE VII. MACHINE DATABASE VALUES OF THE WSCC MODEL

Transmission lines	$X_{T14} = 0.0576pu, X_{T27} = 0.0625pu, X_{T39} = 0.0586pu, X_{T45} = 0.085pu,$ $X_{T46} = 0.092pu, X_{T57} = 0.161pu, X_{T69} = 0.17pu, X_{T78} = 0.072pu,$ $X_{T89} = 0.1008pu, X_{L14} = 0pu, X_{L27} = 0pu, X_{L39} = 0pu, X_{L45} = 0.176pu,$ $X_{L46} = 0.158pu, X_{L57} = 0.306pu, X_{L69} = 0.358pu, X_{L78} = 0.149pu,$ $X_{L89} = 0.209pu,$
Machines	$H_1 = 23.63s, H_2 = 6.4s, H_3 = 3.01s, D = 0.0, T'_{d01} = 8.96s, T'_{d02} = 6.0s,$ $T'_{d03} = 5.89s, T'_{q01} = 0.31s, T'_{q02} = 0.535s, T'_{q03} = 0.6s\, X_{q1}, = 0.0969,$ $X_{q2}, = 0.8645, X_{q3}, = 1.2578, X_{d1} = 0.146, X_{d2} = 0.8958, X_{d3} = 1.3125,$ $X'_{q1} = 0.0969s, X'_{q2} = 0.8645s, X'_{q3} = 1.2578s, X'_{d1} = 0.0608s,$ $X'_{d2} = 0.1198s, X'_{d3} = 0.1813s$
Exciters	$K_{A1} = 20.0, T_{A1} = 0.2s, K_{A2} = 20.0, T_{A2} = 0.2s, K_{A3} = 20.0, T_{A3} = 0.2s$
Operating point information	$P_{G2} = 1.63pu, P_{G3} = 0.85pu, V_1 = 1.04pu, V_2 = 1.025pu, V_3 = 1.025pu$

WSCC, Western System Coordinating Council.

TABLE VIII. CONDITIONS ADOPTED IN MULTI-MACHINE SIMULATION

	Base Condition		**Condition 1**		**Condition 2**	
	P	**Q**	**P**	**Q**	**P**	**Q**
Generator						
G1	0.72	0.27	2.21	1.09	0.36	0.16
G2	1.63	0.07	1.92	0.56	0.80	–0.11
G3	0.85	–0.11	1.28	0.36	0.45	–0.20
Load						
A	1.25	0.50	2.00	0.80	0.65	0.55
B	0.90	0.30	1.80	0.60	0.45	0.35
C	1.00	0.35	1.50	0.60	0.50	0.25

Furthermore, a nonlinear time-domain simulation was carried out. Figure 6 shows the Eigenvalue comparison between NO-PSS and AEO based PSS while Figures 7, 8 and 9 shows the rotor speed, rotor angle and output power response of for the SMIB test system with NO-PSS, GA-based PSS, PSO-based PSS, and AEO-based PSS.

5) Quantitative Performance Evaluation by Comparing with Published Similar Work

To validate the efficiency of the proposed design in comparison with similar works, quantitative results are compared to the reference model in study [9]. Comparing the results of the proposed AEO-design in damping electromechanical oscillations in the SMIB

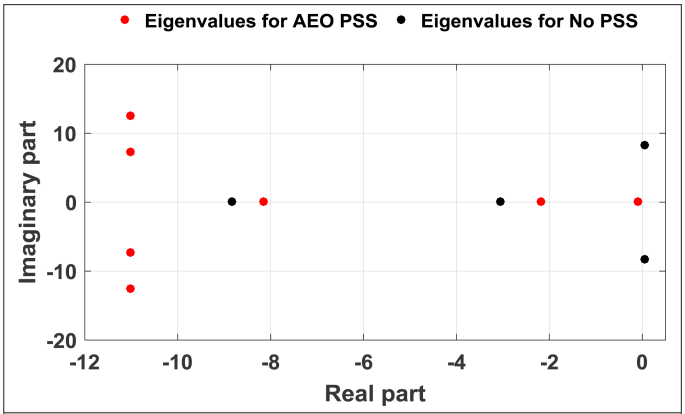

Fig. 6. Eigenvalue plot comparison between AEO-PSS and no-PSS on the system. AEO, artificial eco-system optimization; PSS, power system stabilizer.

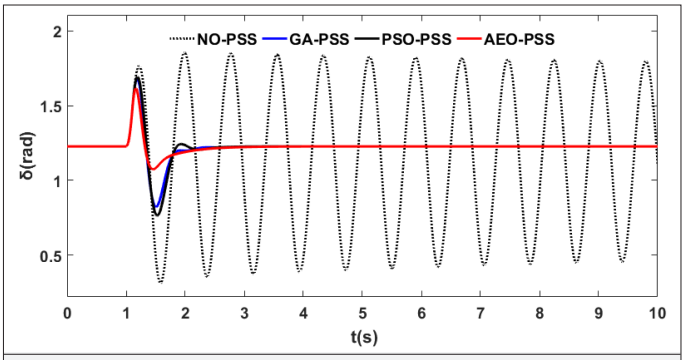

Fig. 7. Rotor angle response of the generator. AEO, artificial eco-system optimization; GA, genetic algorithm; PSO, particle swarm optimization; PSS, power system stabilizer.

test system. Table VI shows the obtained PSS parameters and that obtained in study [9]. Also, the dominant eigenvalue and the damping ratio in percentage for no-PSS, AEO-PSS, and the reference study are shown.

From Table VI, it can be seen that the damping ratio of the dominant eigenvalue was improved from 54.36% to 65.83% compared to the

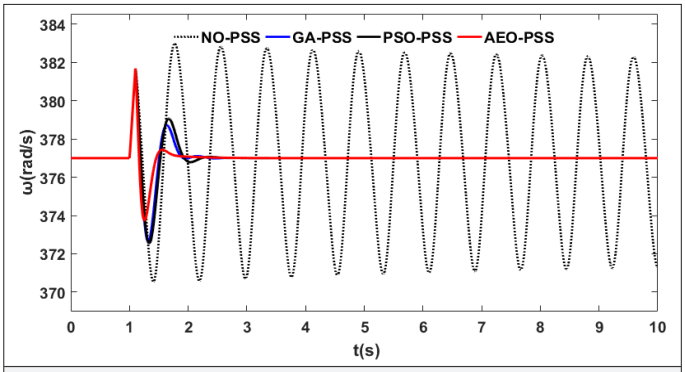

Fig. 8. Rotor speed response of the generator. AEO, artificial eco-system optimization; GA, genetic algorithm; PSO, particle swarm optimization; PSS, power system stabilizer.

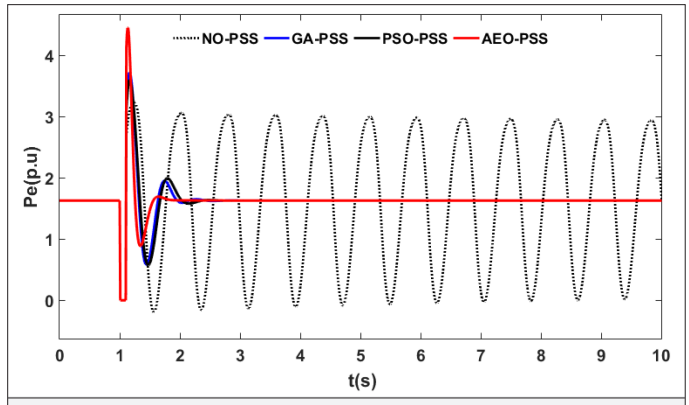

Fig. 9. Active power response of the generator. AEO, artificial eco-system optimization; GA, genetic algorithm; PSO, particle swarm optimization; PSS, power system stabilizer.

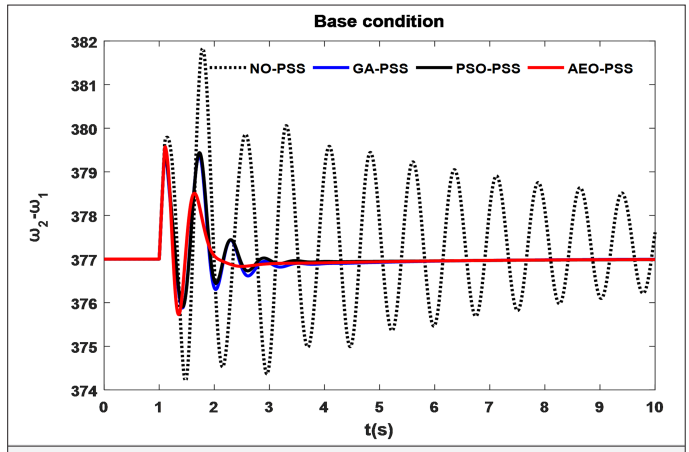

Fig. 10a. Rotor speed response of generator 2 with reference to generator 1 for base condition in Table VIII.

reference study; this is an 11.47% efficiency increase in the damping of electromechanical oscillation.

D. Multi-machine Power System

1) Western System Coordinating Council (WSCC)

Here, a WSCC multi-machine test power system is considered. Whose result was evaluated using GA-based PSS and PSO-based PSS. The optimization process was terminated after 100 iterations for all three algorithms in a population search space of 100 just like in the single machine. Table VII shows the machine database values of the WSCC model, while Table VIII shows the conditions adopted during the simulation process.

Figures 10-16 shows the rotor speed response of generators 2 and 3 with reference to generator 1 for no-PSS, GA-based PSS, PSO-based PSS, and AEO-based PSS as regards the operating conditions in Table VIII.

IV. CONCLUSION

This research considered the optimal design of a PSS for LFO damping in an SMIB and multi-machine power test systems. The differential algebraic equations (DAEs) were used to model the test systems, dynamic and small signal stability analyses were carried out in the

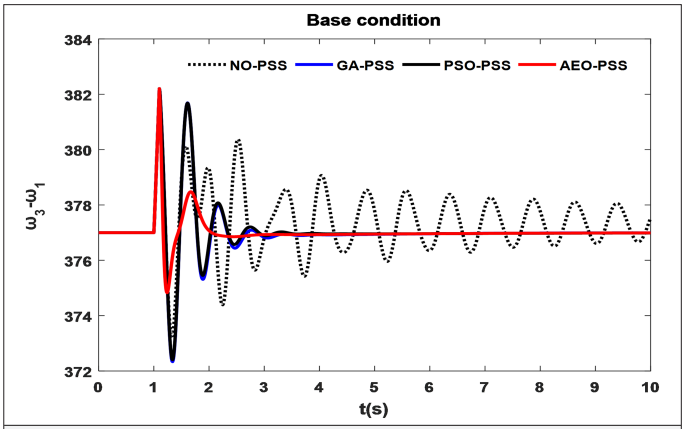

Fig. 10b. Rotor speed response of generator 3 with reference to generator 1 for base condition in Table VIII.

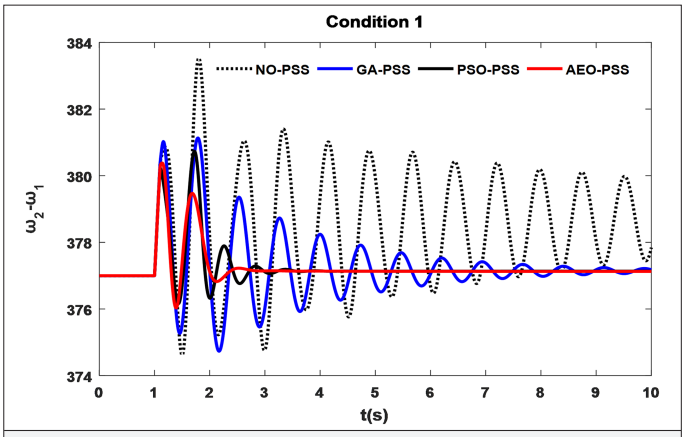

Fig. 11a. Rotor speed response of generator 2 with reference to generator 1 for condition 1 in Table VIII.

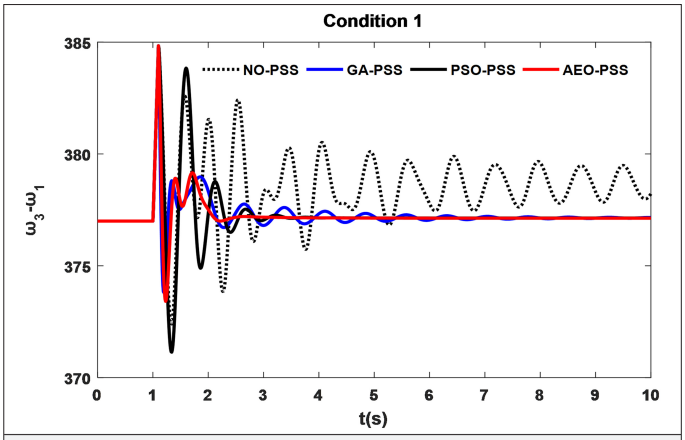

Fig. 11b. Rotor speed response of generator 3 with reference to generator 1 for condition 1 in Table VIII.

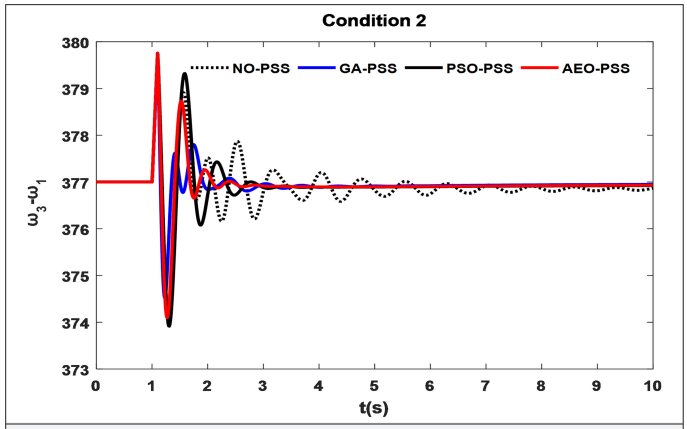

Fig. 12a. Rotor speed response of generator 2 with reference to generator 1 for condition 2 in Table VIII.

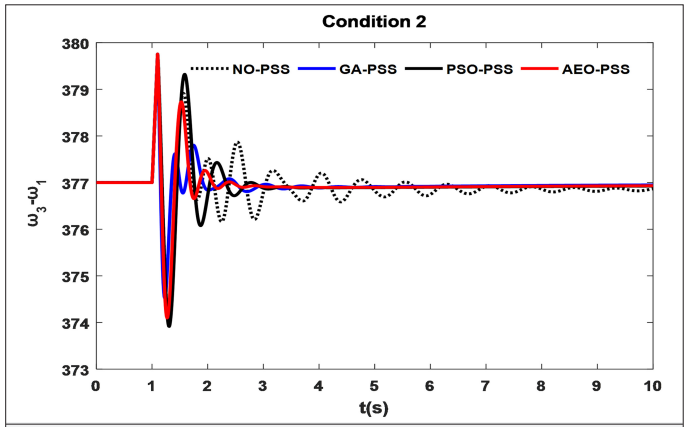

Fig. 12b. Rotor speed response of generator 3 with reference to generator 1 for condition 2 in Table VIII.

design of PSSs. A novel metaheuristic algorithm AEO was adopted in the PSS design, and its performance was evaluated with GA-based PSS, PSO-based PSS, and similar published works to access the proposed AEO-based PSS robustness. Eigenvalue objective function was defined in PSSs design, which shifted the eigenvalues to the left region of the complex s-plane. Three case studies were performed in each test system considering different operating conditions to further validate the AEO-based PSS. Conclusively, the obtained results validate the proposed AEO-based PSS for LFO damping.

Peer-review: Externally peer-reviewed.

Author Contributions: Concept – A.S.; Design – A.S., T.E.O.; Supervision – A.S., N.I.A.W.; Materials – A.S., T.E.O.; Data Collection and/or Processing – A.S., T.E.O.; Analysis and/or Interpretation – A.S., N.I.A.W.; Literature Review – A.S., N.I.A.W.; Writing – A.S., T.E.O.; Critical Review – A.S., N.I.A.W.

Declaration of Interests: The authors declare that they have no competing interest.

Funding: The authors declared that this study has received no financial support.

REFERENCES

1. A. Sabo, N. I. Abdul Wahab, M. L. Othman, M. Z. A. Mohd Jaffar, and H. Beiranvand, "Optimal design of power system stabilizer for multimachine power system using farmland fertility algorithm," *Int. Trans. Electr. Energy Syst.*, vol. 30, no. 12, p. e12657, 2020. [CrossRef]
2. S. Ekinci, D. İzci, and B. Hekimoğlu, "Implementing the Henry gas solubility optimization algorithm for optimal power system stabilizer design," *Electrica*, vol. 21, no. 2, pp. 250–258, 2021. [CrossRef]

3. A. Sabo, N. I. A. Wahab, M. L. Othman, M. Z. A. Jaffar, H. Acikgoz, and H. Beiranvand, "Application of neuro-fuzzy controller to replace SMIB and interconnected multi-machine power system stabilizers," *Sustainability*, vol. 12, no. 22, 2020. [CrossRef]
4. A. Sabo, N. I. Abdul Wahab, and M. Lutfi Othman, "Coordinated design of PSS and IPFC using FFA to control low frequency oscillations," 19th Student Conference on Research and Development (SCOReD). IEEE Publications, 2021, pp. 201–206. [CrossRef]
5. A. Sabo, N. I. A. Wahab, M. L. Othman, M. Zurwatul, and A. M. Jaffar, "Novel farmland fertility algorithm based PIDPSS design for SMIB angular stability enhancement," *Int. J. Adv. Sci. Technol.*, vol. 29, no. 6, pp. 873–882, 2020.
6. S. Ekinci, A. Demiroren, and B. Hekimoglu, "Parameter optimization of power system stabilizers via kidney-inspired algorithm," *Trans. Inst. Meas. Control*, vol. 41, no. 5, pp. 1405–1417, 2019. [CrossRef]
7. H. Beiranvand, and E. Rokrok, "General relativity search algorithm: A global optimization approach," *Int. J. Comput. Intell. Appl.*, vol. 14, no. 3, p. 1550017, 2015. [CrossRef]
8. R. Devarapalli, and B. Bhattacharyya, "Optimal controller parameter tuning of PSS using sine-cosine algorithm," in *Metaheuristic and Evolutionary Computation: Algorithms and Applications*. Berlin: Springer, 2021, pp. 337–360. [CrossRef]
9. I. Davut, "A novel modified arithmetic optimization algorithm for power system stabilizer design," *Sigma J. Eng. Nat. Sci.*, vol. 40, no. 3, pp. 529–541, 2022.
10. M. A. El-Dabah, S. Kamel, M. Khamies, H. Shahinzadeh, and G. B. Gharehpetian, "Artificial gorilla troops optimizer for optimum tuning of TID based power system stabilizer," in 9th Iranian Joint Congress on Fuzzy and Intelligent Systems (CFIS), Vol. 2022, 2022, pp. 1–5. [CrossRef]
11. D. Chitara, K. R. Niazi, A. Swarnkar, and N. Gupta, "Cuckoo search optimization algorithm for designing of a multimachine power system stabilizer," *IEEE Trans. Ind. Appl.*, vol. 54, no. 4, pp. 3056–3065, 2018. [CrossRef]
12. L. Chaib, A. Choucha, S. Arif, H. G. Zaini, A. El-Fergany, and S. S. M. Ghoneim, "Robust design of power system stabilizers using improved harris hawk optimizer for interconnected power system," *Sustainability*, vol. 13, no. 21, p. 11776, 2021. [CrossRef]
13. N. Nahak, and O. Satapathy, " Investigation and damping of electromechanical oscillations for grid integrated micro grid by a novel coordinated governor-fractional power system stabilizer," *Energy Sources Part Recover Util. Environ. Eff.*, pp. 1–29, 2021. [CrossRef]
14. N. Nahak, and S. Satapathy, *A Coordinated Pumped Storage Dual Compensated Hydro Governor with PSS Action to Damp Electromechanical Power Oscillations*, International Transactions on Electrical Energy Systems, vol. 2022, Article ID 8802143, 24 pages, 2022. [CrossRef]
15. S. Satapathy, A. G. Patel, B. Samal, N. Nahak, and P. Nayak, *Design of Optimal Multi-band PSS for Variable Solar-Penetrated Power System BT - Innovation in Electrical Power Engineering, Communication, and Computing Technology*, 2022, pp. 255–267.
16. N. Nahak, O. Satapathy, and P. Sengupta, "A new optimal static synchronous series compensator-governor control action for small signal stability enhancement of random renewable penetrated hydro-dominated power system," *Optim. Control. Appl. Methods*, vol. 43, no. 3, pp. 593–617, 2022. [CrossRef]
17. S. Bohidar, N. Nahak, and R. K. Mallick, "Improvement of Dynamic Stability of power system by Optimal Interline Power Flow Controller," in, 2019, *Innovations in Power and Advanced Computing Technologies*, vol. 1, pp. 1–5. [CrossRef]
18. W. Zhao, L. Wang, and Z. Zhang, "Artificial ecosystem-based optimization: A novel nature-inspired meta-heuristic algorithm," *Neural Comput. Appl.*, vol. 32, no. 13, pp. 9383–9425, 2020. [CrossRef]
19. M. A. El-Dabah, R. A. El-Sehiemy, M. Becherif, and M. A. Ebrahim, "Parameter estimation of triple diode photovoltaic model using an artificial ecosystem-based optimizer," *Int. Trans. Electr. Energy Syst.*, vol. 31, no. 11, p. e13043, 2021. [CrossRef]
20. D. Izci, B. Hekimoğlu, and S. Ekinci, "A new artificial ecosystem-based optimization integrated with Nelder-Mead method for PID controller design of buck converter," *Alex. Eng. J.*, vol. 61, no. 3, pp. 2030–2044, 2022. [CrossRef]
21. M. H. Hassan, S. Kamel, S. Q. Salih, T. Khurshaid, and M. Ebeed, "Developing chaotic artificial ecosystem-based optimization algorithm for combined economic emission dispatch," *IEEE Access*, vol. 9, pp. 51146–51165, 2021. [CrossRef]
22. M. A. Pai, P. W. Sauer, and J. H. Chow, *Power System Dynamics and Stability With Synchrophasor Measurement and Power System Toolbox*, 2nd edn. IEEE Press Wiley, 2018, pp. 1–364.
23. A. Sabo, N. I. A. Wahab, M. L. Othman, M. Z. A. M. Jaffar, and H. Beiranvand, "Farmland fertility optimization for designing of interconnected multi-machine power system stabilizer," *Appl. Model. Simul.*, vol. 4, pp. 183–201, 2020.
24. A. Sabo, N. I. Abdul Wahab, M. L. Othman, M. Z. A. Mohd Jaffar, H. Beiranvand, and H. Acikgoz, "Application of a neuro-fuzzy controller for single machine infinite bus power system to damp low-frequency oscillations," *Trans. Inst. Meas. Control*, vol. 43, no. 16, pp. 3633–3646, 2021. [CrossRef]
25. T. E. Odoh, A. Sabo, and N. I. A. Wahab, "Mitigation of power system oscillation in a DFIG-wind integrated grid: A review," *Appl. Model. Simul.*, vol. 6, pp. 134–149, 2022.
26. A. Sabo, B. Y. Kolapo, T. E. Odoh, M. Dyari, N. I. A. Wahab, and V. Veerasamy, "Solar, wind and their hybridization integration for multi-machine power system oscillation controllers optimization: A review," *Energies*, vol. 16, no. 1, 2023. [CrossRef]

Engr. Dr. Sabo Aliyu (Ph.D) MIEEE. PES. (Member, IEEE) Engr. Dr. Sabo Aliyu completed his Bachelor's degree in Electrical Engineering from the Prestigious Ahmadu Bello University, Zaria, Kaduna State, Nigeria in 2011. Engr. Dr. Sabo Aliyu completed his M.Sc and Ph.D Degrees in Electrical Power Systems Engineering from Universiti Putra Malaysia. His main research areas include the application of Neuro-Fuzzy Controller to power system, Computational Intelligence techniques, Power System Oscillation Damping Controller Designs, Power Systems Optimizations, Power Flow and Optimal Power Flow, Power Quality, and Robust controllers with several online publications. Engr. Dr. Sabo Aliyu is currently a Senior Lecturer at Nigerian Defence Academy, Kaduna State, Nigeria. He is a registered Engineer under the Council for the Regulation of Engineering in Nigeria (COREN).

Theophilus, Ebuka Odoh completed his Bachelor's degree in Electrical and Electronic Engineering from Enugu State University of Science and Technology, Agbani, Nigeria in 2018. He also completed his master's in Electrical and Electronic Engineering (power and machines major) at the Department of Electrical and Electronic Engineering, Nigerian Defence Academy, Kaduna State, Nigeria in 2023. He is a graduate member of the Nigerian Society of Engineers (NSE) and the International Association of Engineers (IAENG). As an early-stage researcher, he is willing to collaborate on developing Intelligent damping controllers, power electronic converters design, control, and optimization, renewable energy integration, and energy storage systems (batteries).

Noor Izzri Abdul Wahab (Senior Member, IEEE) graduated from the University Of Manchester Institute Of Science and Technology (UMIST), UK, in Electrical and Electronic Engineering in 1998, received his MSc in Electrical Power Engineering from the Universiti Putra Malaysia (UPM) in 2002 and his PhD in Electrical, Electronic and System Engineering from Universiti Kebangsaan Malaysia (UKM) in 2010. He is an Associate Professor at UPM's Faculty of Engineering's Department of Electrical and Electronic Engineering. He now has over 100 publications to his name (Journals: 20 local, 40 international, Conference papers: 30 local, 20 international). He is a researcher at UPM's Centre for Advanced Power and Energy Research (CAPER) and an associate member of the UPM's Centre of Electromagnetic and Lightning Protection Research (CELP). He is a Chartered Engineer with the Engineering Council of the United Kingdom and the Institution of Engineering and Technology (IET) of the United Kingdom, as well as a Professional Engineer (Ir.) with the Board of Engineers Malaysia (BEM) and a member of The Institution of Engineers Malaysia (IEM), A senior member of IEEE, a member of the IEEE Power and Energy Society (IEEE-PES), an IEEE Computational Intelligence Society (IEEE-CIS), a member of the Institution of Engineering and Technology (IET) UK, and an International Rough Set Society member (IRSS). His research interests include power system stability (both dynamic and control), artificial intelligence applications in power systems, and power system quality.